Autophagy is suppressed in peripheral blood mononuclear cells during chronic obstructive pulmonary disease.

Authors:

James M Cooper[1*], Shiye Chen[2*], Susan E Lester[1,3], Julia Kim[4], Jason Gummow[1], Tom Crowhurst[4], Emily Lawton[1,4], Arash Badiei[1,4], Phan T Nguyen[1,4], Hubertus PA Jersmann[1,4], Eugene Roscioli[1,4,6 ‡].

Affiliations

[1]Adelaide Medical School, University of Adelaide, Adelaide, SA, Australia.

[2]Biological Sciences School, University of Adelaide, Adelaide, SA, Australia.

[3]Department of Rheumatology, The Queen, Elizabeth Hospital, Adelaide, SA, Australia.

[4]Department of Thoracic Medicine, Royal Adelaide Hospital, Adelaide, SA, Australia.

[5]Centre for Cancer Biology, SA Pathology and University of South Australia, Adelaide, SA, Australia

*Authors contributed equally

‡ Correspondence: Eugene Roscioli
Adelaide Health and Medical Science
Building, Corner of North Terrace and
George St, Adelaide 5005, South
Australia, Australia
Tel +61 8 8313 7088
Email: Eugene.Roscioli@adelaide.edu.au

Abstract:

Assessing autophagy promises to provide valuable information regarding the pathogenesis of chronic obstructive pulmonary disease (COPD). However, measuring the dynamic aspect of autophagy is challenging, and sample manipulation can cause signal fluctuations that deviate from the situation *in vivo*. Our aim was to assess an organotypic method to quantify autophagy in the context of COPD, where autophagy has demonstrated disease-related modulation. Blood from control and COPD participants was treated with/out chloroquine. Protein from peripheral blood mononuclear cells (PBMC) was then isolated and compared for LC3B-II abundance. Our observations show that while basal level LC3B-II abundance was similar between each group ($P = 0.60$), autophagic flux was significantly lower in the COPD cohort, suggesting disruption in autophagy ($P = 0.004$). We aim to extend this inquiry and compare pulmonary vs blood samples, to identify the utility of measuring autophagy in blood as a diagnostic outcome predictive of early COPD.

Short title:

Reduced autophagy in COPD

Key words:

Autophagic flux; Biochemistry; Diagnostic; LC3; Lymphocyte; Respiratory.

Introduction

Chronic obstructive pulmonary disease (**COPD**) is a member of the group of conditions in which dysregulated macroautophagy (hereafter referred to as autophagy), is understood to potentiate this disease and may have a role in causation. Many disease phenotypes synonymous with COPD including the autoimmune-like inflammation [1], infection [2] and accelerated senescence [3], align with aberrations in the processes which rely on normal autophagy. Despite these findings, there remains an important debate to determine whether autophagic flux is accelerated as a maladaptive response, or disrupted, thereby diminishing the homeostatic support imparted by this enigmatic biochemical process (reviewed in [4]). In broad terms, this uncertainty is because COPD is complex and typically diagnosed at an advanced stage when the convergence of numerous pathophysiological events obscure discrete molecular patterns. Coupled to this, assessing autophagy function in a manner that reliably reflects the *in vivo* situation, is a significant challenge and requires careful consideration [5]. Hence, despite the significant promise of targeting autophagy to manage COPD, which is the world's third most lethal disease [6], autophagy remains disconnected from clinical and pharmacological inquiry.

Addressing the measurement problem, a recent investigation has described an organotypic method to assess autophagy function in peripheral blood mononuclear cells (**PBMC**), by directly treating blood samples with/out chloroquine (**CQ**) and assessing readouts of LC3B-II [7]. The value of this method is that the *ex vivo* measures of autophagic flux approximate the situation in the participant's PBMCs; taking blood requires minimal clinical resource, the period from collection to protein isolation is brief, and the blood maintains the PBMCs as if they were still in the body. While the lethal process ascribed to COPD occur in the airways, this condition is synonymous with serious systemic effects [8]. Further, the products of inflammation and inhaled environmental factors (e.g. chemicals from tobacco and occupational/environmental exposures), are transmitted to cells of the circulatory system [9, 10]. In line with this, COPD exhibits an influential genetic component [11]. Consequently, immune cells that encode susceptibility genes can be negatively affected by the risk factors locally in the pulmonary system, as well as those that persist in the systemic circulation. Autophagy-related genes are linked (or are convincing candidates) to the development of human disease, including COPD, asthma and pulmonary fibrosis [12], and we are now identifying the relationship between the peripheral consequences of COPD and dysregulation of autophagy [13-15]. Hence, an interesting question that arises from these findings is whether assessing autophagy in the peripheral circulation can inform the development of a non-invasive screen for COPD.

Here we assessed autophagy in PBMCs isolated from individuals suffering from COPD, to evaluate alterations in autophagic flux. Our observations show that PBMCs from participants with COPD exhibit disruption in autophagy when compared to the outcomes from healthy controls.

Results

PBMC from COPD participants exhibited reduced autophagic flux.

The observations for LC3B-II protein abundance were first compared separately for each group/exposure (**Fig. 1A-B**). PBMCs from either group exhibited a similar near-zero signal distribution for the untreated condition ($P = 0.60$, control vs COPD), indicating low basal LC3B-I lipidation for PBMCs is normal for these groups. Both control and COPD cells also demonstrated an elevation in LC3B-II abundance after exposure to CQ (both $P < 0.001$, CQ vs NT). However, control PBMCs accumulated an appreciably larger amount of LC3B-II in response to CQ over the exposure interval (P

< 0.007, control vs COPD), suggesting that PBMCs from COPD have some restriction in the processes leading to LC3B-I lipidation. Values for autophagic flux (△LC3B-II) were derived by determining the difference between LC3B-II signals for the CQ and NT exposures, within groups. Shown in **Fig. 1C**, the COPD group exhibited significant autophagy insufficiency when compared to the control group (P = 0.004, control vs COPD). The observations for autophagic flux were further assessed to determine whether differences in age and gender (see **Table 2**), were significant confounding variables (model-based analysis). Shown in **Table 1**, the reduction in autophagic flux determined for the COPD group remained significant after accounting for the covariates (i.e. significant after age/gender adjustment; P=0.003, COPD vs control). However, estimates derived within the model show that age (gender was a non-significant confounder), can influence outcomes related to autophagic flux. The efficacy/specificity of the LC3B-I/II antibody was also assessed using lentivirus CRISPR KO directed to *ATG5*. Depletion of ATG5 protein caused a reduction in ATG5-mediated lipidation of LC3B-I (i.e. a reduction in LC3B-II), concomitant with an elevated abundance of Sequestosome-1 (**Fig. 1D**).

Table 1: Model-based analysis of autophagic flux adjusted for age and gender.

Covariates	ΔLC3B-II:Actin-β (95% CI)		COPD vs Controls
	COPD	Controls	P value
None	0.37 (-0.01, 0.76)	0.82 (0.42, 1.23)	<0.0001
Age, Sex [1]	0.35 (-0.03, 0.73)	0.59 (0.24, 0.94)	0.003

[1]Estimated at the covariate distribution of COPD patients i.e. the predicted values if controls had been age/sex matched to COPD patients.

Methods

Participants

Ethics approval was granted by the Central Adelaide Local Health Network Human Research Ethics Committee (CALHN reference number: 12978). Peripheral blood was obtained by the clinical team at the Royal Adelaide Hospital's Department of Thoracic Medicine and Queen Elizabeth Hospital's Respiratory Medicine Unit. Participant demographics are shown in **Table 2**. Control participants reported no history of chronic respiratory disease and were never smokers. COPD was determined by clinical observations and lung function test (FEV1/FVC ratio below 70%).

Table 2: Participant demographics.

	n	Age (SD)	Gender (F / M)	FEV1/FVC % (SD)
Control	15	55.3 (12.7)	6 / 9	78.6 (5.8)
COPD	22	67.4 (6.7)	7 / 15	53.6 (13.5)
Total	37	62.5 (11.2)	13 / 24	63.8 (16.6)

FEV1, forced expiratory volume in one second. FVC, forced vital capacity.

PBMC isolation

PBMC were isolated adhering to (without deviation in processes and products), the optimized method described by Bensalem et al. (2020). Briefly, blood in lithium-heparin tubes were entered into the PBMC isolation process no longer than 2 hours after collection from the clinic. Chloroquine diphosphate was added to a concentration of 150 μM and allowed to incubate for 1 h at 37°C, simultaneously with the untreated sample. PBMC were isolated using the ficoll gradient method and 1x red blood cell lysis applied to clear erythrocytes.

Western blot

Western blots were performed as previously described (e.g. [16]). Briefly, protein was isolated using M-PER Mammalian Protein Extraction Reagent (Thermo Fisher Scientific Inc, 78501), and Halt Protease and Phosphatase Inhibitor Cocktail (Thermo Fisher Scientific Inc, 78441). Protein was quantified using the Pierce BCA Protein Assay Kit (Thermo Fisher Scientific Inc, 23225), and 10 μg electrophoresed in 4–12% Bis-Tris denaturing gels (Thermo Fisher Scientific, NP0321) using MOPS chemistry (Thermo Fisher Scientific, NP0001). Transfer was to 0.2 μm pore PVDF membranes (Bio-Rad Laboratories Inc, 1704156), which were sectioned so corresponding target and normalization signals could be quantified from the same blot (i.e. to mitigate loading inconsistencies due to inter-experimental variation). Membranes were blocked in 5% skim milk for mouse anti-Actin-β (1:10,000, A1978; Sigma-Aldrich Co.), and 5% BSA (Merck, 126575), for rabbit anti-LC3B-I/II (Cell Signaling Technology, 4108), and subsequently probed overnight at 4°C with the same respective buffer/antibodies combinations. Secondary incubation was 1 hour at RT in 5% skim milk with mouse or rabbit IgG horseradish peroxidase-conjugated antibodies (R&D Systems, HAF007 and HAF008, respectively). The suspension for blocking and antibody incubations was 1x Tris buffered saline (Thermo Fisher Scientific, J60877.K3), with 0.1% Tween 20 (Merck, P1379). Chemiluminescent signal production was with Amersham ECL Advanced Western Blotting detection reagents (GE Healthcare, RPN2135). Image acquisition was performed using the LAS-4000 Luminescent Image Analyzer (Fujifilm Life Sciences, Japan), with signal detection set to annotate blots beyond the linear range (depicted by pink-purple color). Histogram densitometry was performed using Multi Gauge software (Fujifilm Life Sciences, V3.1, Japan).

Generation of LentiCRISPRv2-*ATG5*

Briefly, HEK-293T cells were co-transfected with lentivirus construct encoding *Cas9* and a sgRNA targeting exon 7 of *ATG5* (LentiCRISPRv2-*ATG5*; Addgene, 99573 [17]; deposited by Edward Campbell), pMDLg/pRRE (Addgene, 12251), pMD2.G (Addgene, 12259), and pRSV-REV (Addgene, 12253) (Packaging vectors deposited by Didier Trono) using Lipofectamine 3000 (ThermoFisher Scientific, L3000150). Supernatant was collected 24 and 48 hours after transfection, centrifuged at 3000 rpm, filtered (Corning, 430768), and ultra-centrifuged (18000 rpm; ThermoFisher Scientific, Sorvall WX80). After ultra-centrifugation, supernatant was removed and the pellet resuspended and preserved at -80°C. Titration was performed by transducing HEK293T cells in a 24 well plate with LentiCRISPRv2-*ATG5*, and after 72 hours transduction the cells were collected, and DNA extracted/purified. DNA for cells transduced with Lenti GFP was used as a standard ladder and qPCR was performed and normalized to house-keeper gene to determine LentiCRISPRv2-*ATG5* titre.

Generation of ATG5 KO 16HBE14o- cells

The LC3B-I/II antibody applied here is known to be sensitive and specific for LC3B-II [18]. To verify this, 16HBE14o- cells (EMD Millipore Corporation, SCC150), were used to model the functional knockout of autophagy. This cell line was chosen as 16HBE14o- produced high LC3B-1I and low Sequestosome-1 signals during log phase growth (i.e. to

allow sensitive comparison vs outcomes for *ATG5* KO), and to avoid applying clinical samples (i.e. PBMCs), to optimization procedures. 16HBE14o- cells were propagated according to the manufacturers protocol (EMD Millipore Corporation, SCC150) and transduced with LentiCRISPRv2-*ATG5* at an MOI of 10 and allowed to culture for 48 hours. Selective pressure on transduced cells was applied by culturing in the presence puromycin (ThermoFisher Scientific, J67236.XF) for 15 day, after which colonies were selected, propagated and screened. To confirm ATG5 knockout, western blot analysis was performed using anti-rabbit-ATG5 (1:2000; AbCam, Ab108327). Functional inhibition of autophagy was assessed by western blot using LC3B-I/II (as above) and Sequestosome-1 (Cell Signaling Technology, 5114) antibodies.

Statistical analysis

Analysis was performed in Stata v18 (StataCorp LLC). LC3B-II western blot intensities were analyzed using a gamma (log link) multi-level regression model, with log(Actin-β) intensities as an offset and a robust variance-covariance. Random effects included individuals nested within blot, and CQ treatment as a crossed random factor within each individual. Fixed effects included group (COPD, Control), CQ treatment (yes, no) and an interaction term. Postestimation tools were used to estimate marginal means for LC3B-II normalized to Actin-β (LC3B-II:Actin-β), and the differences in these marginal means due to CQ treatment (LC3B-II:Actin-β). Age and sex were included as additional covariates, and a full factorial model was estimated. The marginal means for both COPD and Controls were then estimated using the age/sex covariate distribution of COPD participants i.e. the results for the Controls were estimated according to the same age/sex distribution as COPD participants to allow a direct comparison.

Discussion/Conclusion

We applied the approach developed by Bensalem et al. (2020), to show autophagy is restricted in PBMCs in the context of COPD. This method afforded a temporal window to assess autophagy in an organotypic manner (i.e. *ex vivo* exposure to CQ), which enabled us to quantify and compare the relative magnitude of autophagic function available to PBMCs from control and COPD participants. Comparative reports for COPD and related conditions that exhibit significant systemic inflammation, for the most part, explain the involvement of autophagy in disease processes with only a snapshot of LC3B-II and (but not always) an autophagy-receptor substrate (e.g. [19-22]). This can provide important information but are not sufficient to describe the manner in which the disease-related phenomenon connects to the perturbations in autophagic competency. As flux implies a process (i.e. with a start and endpoint), it is important to consider the dynamic aspect of autophagy to provide information pertinent to autophagic function. Further to this, and important for PBMCs, measures of autophagy receptor abundance do not always correlate with the outcomes for autophagic flux inferred by the abundance of LC3B-II (e.g. [7, 23, 24]). Indeed, we tested three autophagy receptor proteins (NDP52, Optineurin and Sequestosome-1), in addition to phospho-ATG16L1 which is purported to correlate with autophagy induction [25], and neither provided outcomes to support the LC3B-II observations for PBMCs. Undoubtedly, these measurement complexities are central to the current debate as to whether autophagy is inappropriately attenuated or increased as a maladaptive response to the COPD-related disease phenomena. Our findings, at least for PBMCs, point to a scenario whereby those COPD-related phenotypes that can be logically aligned with autophagic dysregulation, arise from inappropriate restriction of autophagic flux.

The utility and limitations of these outcomes can be addressed in terms of whether measures of autophagy can be used as a prospective diagnostic readout for COPD. While assessing blood is an attractive non-invasive tissue for diagnostic

purposes, a central question is whether assessing autophagy in PBMCs is a suitable proxy for the airways. Despite our findings and the increasing evidence that peripheral lymphocytes are altered in COPD [10, 26], the vast airway epithelial and macrophage interface is the first to respond to the majority of COPD-related environmental and microbial exposures. Hence, a rational position is that the assessment of lung tissues should offer more informative predictive insights, particularly for early disease. Indeed, outcomes derived from lung samples have been convincingly shown to exhibit autophagy incompetency in COPD [2, 27, 28]. Further, the abundance of autophagy receptors (to support LC3B-II observations) in e.g. airway epithelial cells, generally correlate with LC3B-II levels, meaning that their analysis can provide a robust assessment of autophagic flux [2]. To address this, we have optimized a model to assess airway samples using an adapted version of the method applied here, and we are now comparing readouts from autologous blood and lung samples (i.e. PBMC vs bronchioalveolar lavage vs airway biopsies). In terms of achieving a balance of disease/control participant demographics, our findings and observations from other groups support the position that chronological age informs (and is influence by), the state of the biochemical processes that regulate autophagy (**Table 1**; [27, 29, 30]). This is demonstrated in COPD, where accelerated senescence and unscheduled apoptosis are hallmarks of disease and are associated with the dysregulation of autophagy [3, 31-33]. While our evaluation of autophagy remained significant after correcting for the age disparity, assessments using homogenous participant groups will be a central prerequisite leading to a diagnostic model that is predictive of COPD.

Underpinning all of this, the evaluation of autophagy is based on semiquantitative protein abundance data from western blot biochemistry. Understanding at the complex nexus between autophagy and COPD (particularly one that offers utility in a clinical setting), awaits more efficient analytical method (i.e. vs Western blot analysis), that generates explicit outcome measures. Another goal is to achieve a clear description of the specific mechanisms that connect autophagic dysregulation with the pathogenesis of COPD. It is our aim to elucidate these mechanisms and align the outcomes with the screening method proposed here, to provide an effective diagnostic tool that is predictive of early COPD before the condition becomes irreversible.

Acknowledgements

We are grateful for the expertise and support of the clinical staff of the Royal Adelaide Hospital Thoracic Department, The Queen Elizabeth Hospital Respiratory Unit and the participants enrolled into this study who generously provided their valuable time and tissue samples. This study was funded by the Royal Adelaide Research Committee, Royal Adelaide Hospital Research Fund, The Health Services Charitable Gifts Board, and the Rebecca L Cooper Medical Research Foundation.

Disclosure statement

The authors have no COI to disclose.

Reference list

1. Huang HQ, Li N, Li DY, et al. Autophagy Promotes Cigarette Smoke-Initiated and Elastin-Driven Bronchitis-Like Airway Inflammation in Mice. *Front Immunol*. 2021;12:594330.

2. Poh WP, Kicic A, Lester SE, et al. COPD-Related Modification to the Airway Epithelium Permits Intracellular Residence of Nontypeable Haemophilus influenzae and May Be Potentiated by Macrolide Arrest of Autophagy. *Int J Chron Obstruct Pulmon Dis*. 2020;15:1253-60.

3. Fujii S, Hara H, Araya J, et al. Insufficient autophagy promotes bronchial epithelial cell senescence in chronic obstructive pulmonary disease. *Oncoimmunology*. 2012;1(5):630-41.

4. Tan WSD, Shen HM, Wong WSF. Dysregulated autophagy in COPD: A pathogenic process to be deciphered. *Pharmacol Res*. 2019;144:1-7.

5. Klionsky DJ, Abdel-Aziz AK, Abdelfatah S, et al. Guidelines for the use and interpretation of assays for monitoring autophagy (4th edition)(1). *Autophagy*. 2021;17(1):1-382.

6. Safiri S, Carson-Chahhoud K, Noori M, et al. Burden of chronic obstructive pulmonary disease and its attributable risk factors in 204 countries and territories, 1990-2019: results from the Global Burden of Disease Study 2019. *BMJ*. 2022;378:e069679.

7. Bensalem J, Hattersley KJ, Hein LK, et al. Measurement of autophagic flux in humans: an optimized method for blood samples. *Autophagy*. 2021;17(10):3238-55.

8. Agusti AG. Systemic effects of chronic obstructive pulmonary disease. *Proc Am Thorac Soc*. 2005;2(4):367-70; discussion 71-2.

9. Barnes PJ. Chronic obstructive pulmonary disease: effects beyond the lungs. *PLoS Med*. 2010;7(3):e1000220.

10. Hodge G, Jersmann H, Holmes M, et al. BLTR1 Is Decreased in Steroid Resistant Pro-Inflammatory CD28nullCD8+ T Lymphocytes in Patients with COPD-The Spillover Hypothesis Explained? *Biology (Basel).* 2023;12(9).

11. Cho MH, Hobbs BD, Silverman EK. Genetics of chronic obstructive pulmonary disease: understanding the pathobiology and heterogeneity of a complex disorder. *Lancet Respir Med.* 2022;10(5):485-96.

12. Yamamoto H, Zhang S, Mizushima N. Autophagy genes in biology and disease. *Nat Rev Genet*. 2023;24(6):382-400.

13. Balnis J, Drake LA, Singer DV, et al. Deaccelerated Myogenesis and Autophagy in Genetically Induced Pulmonary Emphysema. *Am J Respir Cell Mol Biol*. 2022;66(6):623-37.

14. Puig-Vilanova E, Rodriguez DA, Lloreta J, et al. Oxidative stress, redox signaling pathways, and autophagy in cachectic muscles of male patients with advanced COPD and lung cancer. *Free Radic Biol Med*. 2015;79:91-108.

15. Liao SX, Sun PP, Gu YH, et al. Autophagy and pulmonary disease. *Ther Adv Respir Dis*. 2019;13:1753466619890538.

16. Delhove J, Alawami M, Macowan M, et al. Organotypic sinonasal airway culture systems are predictive of the mucociliary phenotype produced by bronchial airway epithelial cells. *Sci Re*p. 2022;12(1):19225.

17. Imam S, Talley S, Nelson RS, et al. TRIM5alpha Degradation via Autophagy Is Not Required for Retroviral Restriction. *J Virol*. 2016;90(7):3400-10.

18. Gottlieb RA, Andres AM, Sin J, et al. Untangling autophagy measurements: all fluxed up. *Circ Res.* 2015;116(3):504-14.

19. Wu Y, Xu B, He X, et al. Correlation between autophagy levels in peripheral blood mononuclear cells and clinical parameters in patients with chronic obstructive pulmonary disease. *Mol Med Rep*. 2018;17(6):8003-9.
20. An N, Chen Y, Wang C, et al. Chloroquine Autophagic Inhibition Rebalances Th17/Treg-Mediated Immunity and Ameliorates Systemic Lupus Erythematosus. *Cell Physiol Biochem*. 2017;44(1):412-22.
21. Vomero M, Manganelli V, Barbati C, et al. Reduction of autophagy and increase in apoptosis correlates with a favorable clinical outcome in patients with rheumatoid arthritis treated with anti-TNF drugs. *Arthritis Res Ther*. 2019;21(1):39.
22. RostamiRad A, Ebrahimi SSS, Sadeghi A, et al. Palmitate-induced impairment of autophagy turnover leads to increased apoptosis and inflammation in peripheral blood mononuclear cells. *Immunobiology*. 2018;223(3):269-78.
23. Shi X, Lai C, Zhao L, et al. Chloroquine and Rapamycin Augment Interleukin-37 Expression via the LC3, ERK, and AP-1 Axis in the Presence of Lipopolysaccharides. *J Immunol Res*. 2020;2020:6457879.
24. Lin LC, Chang HY, Kuo TT, et al. Oxidative stress mediates the inhibitory effects of Manzamine A on uterine leiomyoma cell proliferation and extracellular matrix deposition via SOAT inhibition. *Redox Biol*. 2023;66:102861.
25. Tian W, Alsaadi R, Guo Z, et al. An antibody for analysis of autophagy induction. *Nat Methods*. 2020;17(2):232-9.
26. Oudijk EJ, Lammers JW, Koenderman L. Systemic inflammation in chronic obstructive pulmonary disease. *Eur Respir J Suppl*. 2003;46:5s-13s.
27. Kuwano K, Araya J, Hara H, et al. Cellular senescence and autophagy in the pathogenesis of chronic obstructive pulmonary disease (COPD) and idiopathic pulmonary fibrosis (IPF). *Respir Investig*. 2016;54(6):397-406.
28. Albano GD, Montalbano AM, Gagliardo R, et al. Autophagy/Mitophagy in Airway Diseases: Impact of Oxidative Stress on Epithelial Cells. *Biomolecules*. 2023;13(8).
29. Yoon YS, Jin M, Sin DD. Accelerated lung aging and chronic obstructive pulmonary disease. *Expert Rev Respir Med*. 2019;13(4):369-80.
30. Cuervo AM, Bergamini E, Brunk UT, et al. Autophagy and aging: the importance of maintaining "clean" cells. *Autophagy*. 2005;1(3):131-40.
31. Grosjean I, Romeo B, Domdom MA, et al. Autophagopathies: from autophagy gene polymorphisms to precision medicine for human diseases. *Autophagy*. 2022;18(11):2519-36.
32. Jeong YJ, Lee KH, Woo J, et al. Downregulation of Lysosome-Associated Membrane Protein-2A Contributes to the Pathogenesis of COPD. *Int J Chron Obstruct Pulmon Dis*. 2023;18:289-303.
33. Jiang H, Xu Y, Jiang Y, et al. FOXO3 Activation Prevents Cellular Senescence in Emphysema Induced by Cigarette Smoke. *COPD*. 2023:1-12.

Figure legend.

Figure 1. Peripheral blood mononuclear cells from individuals with COPD exhibited reduced autophagic flux. (**A**) Basal level LC3B-II observation densities show a near-zero distribution for both groups, while the COPD group exhibited a significant reduction in LC3B-II accumulation with chloroquine (QC), vs the controls. (**B**) A representative blot (n=6 in total) comparing no-treatment and CQ outcomes for LC3B-I/II and Actin-β (ACTB). **C**). Measures of autophagic flux (△LC3B-II) showed a significant reduction in autophagic competency for the COPD group. (**D**) The LC3B-I/II antibody was validated using protein isolated from 16HBE14o- cells transduced with a CRISPR *ATG5* KO construct. As expected, the depletion of ATG5 caused a large reduction in the LC3B-II signal (the lipidated form of LC3B-I), and substantial increases in the LC3B-I and p62/Sequestosome-1 (SQSTM1) signals. Pink-purple color within the LC3B-I and Sequestosome-1/p62 blots indicate signal saturation beyond the linear range determined for these proteins.

*Outcomes for LC3B-II were normalized to the Actin-β signal. Control, n=16 and COPD, n= 22. "**" denoted P < 0.01. Outcomes for the violin graphs were from non-parametric analyses; Wilcoxon matched pairs rank were used when comparing no-treatment and CQ, and Kruskall-Wallis rank test for comparisons between control vs COPD. Violin graphs boxplots show ± standard error and whiskers denote ± 95% CI.*

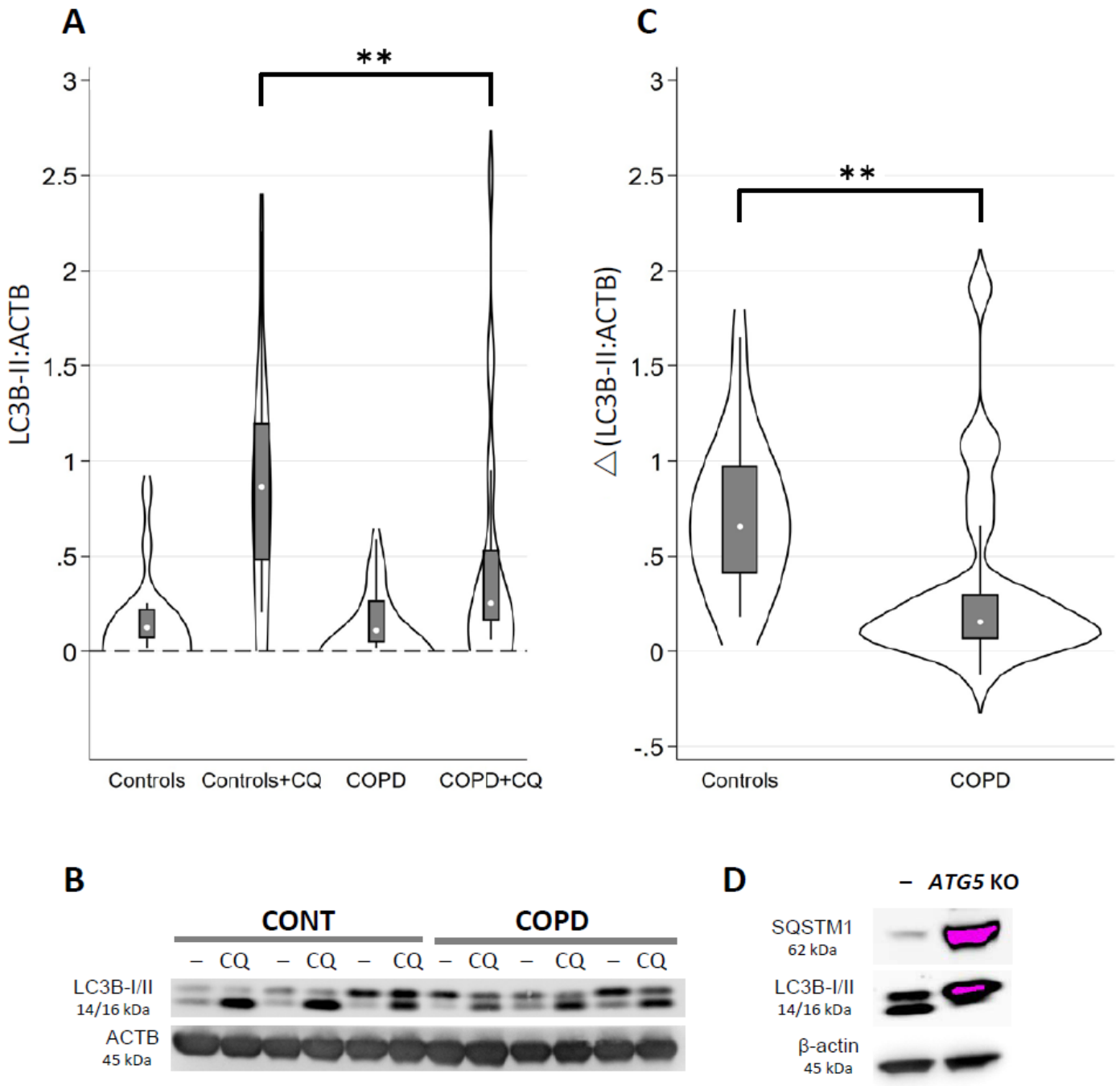
A
**
LC3B-II:ACTB
3
2.5
2
1.5
1
.5
0
Controls
Controls+CQ
COPD
COPD+CQ
C
**
△(LC3B-II:ACTB)
3
2.5
2
1.5
1
.5
0
-.5
Controls
COPD
B
CONT
COPD
– CQ – CQ – CQ – CQ – CQ – CQ
LC3B-I/II
14/16 kDa
ACTB
45 kDa
D
– ATG5 KO
SQSTM1
62 kDa
LC3B-I/II
14/16 kDa
β-actin
45 kDa